Vis Comput
DOI 10.1007/s00371-015-1194-8

ORIGINAL ARTICLE

Mass spring models with adjustable Poisson's ratio

Maciej Kot[1] · **Hiroshi Nagahashi**[1]

Abstract In this paper we show how to construct mass spring models for the representation of homogeneous isotropic elastic materials with adjustable Poisson's ratio. Classical formulation of elasticity on mass spring models leads to the result, that while materials with any value of Young's modulus can be modeled reliably, only fixed value of Poisson's ratio is possible. We show how to extend the conventional model to overcome this limitation. The technique is demonstrated on cubic lattice as well as disordered networks.

Keywords Mass spring model · Soft body deformation · Physically based modeling

1 Introduction

Computer graphics community has been using mass spring models (MSMs) for the representation of deformable objects since the earliest attempts to accommodate elastic solids in computer-generated animations. The ability to simulate the behavior of such objects not only benefits the animations, which become richer and more realistic, but also opens new possibilities for games (in terms of gameplay) and virtual reality applications. While MSMs were popular because of their low implantation complexity, the link between their physical properties and spring-network parameters has never been properly established. This led to a belief that MSMs cannot represent elastic objects accurately and that the models do not converge to certain solutions upon mesh refinement [8,13]. Consequently more physically accurate techniques such as finite element method (FEM) gained popularity.

The accuracy of the description of an elastic object is, however, not a problem in MSM representations. The standard lattice-based models used in physics, mechanical engineering and other related fields offer a description of elastic solids which is as accurate as the limitations of linear elasticity theory allow it to be [3,4,9]. There is, however, a limitation to what can be modeled with MSMs. While any value of Young's modulus E can be obtained with classical models, Poisson's ratio ν is limited to 1/4 for volumetric objects and 1/3 for 2D meshes. This allows to freely adjust the stiffness of an object, but is not sufficient to replicate all types of materials. In this work we show how to efficiently extend conventional MSM to overcome this limitation and obtain a reliable model of any homogeneous isotropic solid. Achieving a realistic and fast MSM behavior based on physical laws is especially useful for VR applications, where interaction with the environment is a common problem.

This work investigates only the static properties of MSMs. We do not address here the question of how these systems evolve over time or what are the most efficient numerical schemes to track their dynamics. Efficient ways of simulating the dynamics can be found, e.g., in [6,10].

2 Mass spring models

The present work is a continuation of [3], where basic properties of mass spring models have been discussed. Below we summarize the most important results; however, the reader is encouraged to refer to [3] for a more detailed introduction.

If we consider a homogeneous isotropic solid, its elastic properties are defined by exactly two parameters (elastic moduli). Classically Young's modulus E and Poisson's ratio ν are the popular pair. The Young's modulus is the ratio

✉ Maciej Kot
eustachy@gmail.com

[1] Imaging Science and Engineering Laboratory, Tokyo Institute of Technology, Tokyo, Japan

Published online: 08 December 2015

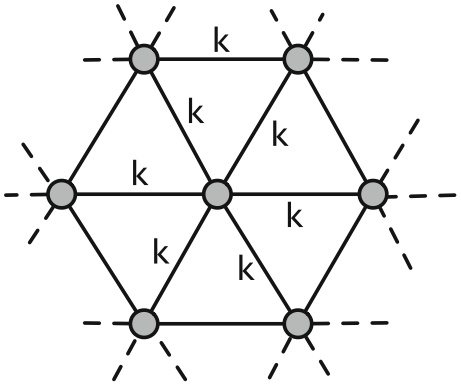

Fig. 1 Hexagonal lattice

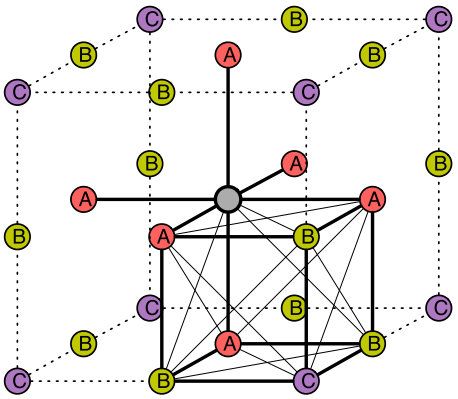

Fig. 2 Cubic lattice. The nearest neighbors of a node are classified into three groups *A*, *B* and *C*. They correspond to the potential connections along *cube edges*, *face diagonals* and *cube diagonals*

of stress to strain measured along the same axis under an uniaxial stress condition, that is, it gives the resistance to directional stretching or compression. The Poisson's ratio is the ratio of transverse to axial strain (denotes to what degree material expands in one direction when compressed in another). Depending on the application, besides E and ν, other moduli are often used such as bulk modulus K, or Lamé parameters λ and μ. In any description only two of them are independent and providing a link between spring-network parameters, and a chosen pair of the elastic moduli is sufficient to describe elastic properties of the MSM.

In case of 2D MSM, an isotropic homogeneous structure can be obtained with hexagonal lattice (Fig. 1) [9]. All the springs have the same spring coefficient k and the relation between the spring coefficient and the Lamé constants for such network is given by

$$\lambda = \mu = \frac{3}{4\sqrt{3}}k, \tag{1}$$

from which it follows that $E = \frac{2}{\sqrt{3}}k$ and $\nu = \frac{1}{3}$. Springs are assumed to be of a unit length.

Similarly a volumetric isotropic solid can be constructed with cubic lattice MSM [4]. The spring connections exist between nearest neighbors (A) and second nearest neighbors (B) (Fig. 2) and all have the same spring coefficient k. The elastic moduli for such network are given by

$$E = 2.5\frac{k}{a} \quad \nu = 1/4, \tag{2}$$

where a is the length of an edge of an elemental cube.

A more general description of MSMs can be obtained from their statistical properties [3]. For a given volume V of a material represented by an MSM with springs of lengths L_i and stiffness coefficients k_i, the bulk modulus is given by

$$K = \frac{1}{9V}\sum_i k_i L_i^2. \tag{3}$$

This can be used to estimate elastic moduli not only of lattice-based MSMs, but also disordered networks, giving in such case approximations which are expected to hold as long as the network remains reasonably homogeneous.

The models listed above have a limitation on the value of Poisson's ratio, which comes from a well-established result of the continuum mechanics. If the constituents of a material interact with the central forces dependent upon distance alone the Poisson's ratio of a homogeneous and isotropic material is identically 1/4 (or 1/3 for a 2D system) [5,7]. Other values of the Poisson's ratio can be obtained by incorporating non-central forces into the model, e.g., the angular terms, or forces that do not depend on distance alone or by introducing anisotropy [5].

An example of such extension is the Kirkwood model of an isotropic 2D material [9]. It is based on a hexagonal lattice and introduces additional angular springs, which provide a resisting force when an angle between two coinciding springs changes from its neutral value of 60° (Fig. 3).

The Poisson's ratio is given by

$$\nu_{2D} = \left(1 - \frac{3\beta}{2ka^2}\right) \Big/ \left(3 + \frac{3\beta}{2ka^2}\right), \tag{4}$$

where a is the length of an edge of a triangle, k is a spring stiffness coefficient of regular springs and β of angular springs.

Similar modifications are possible in case of 3D materials and the problem of constructing MSM-like models capable of representing isotropic materials with arbitrary values of Poisson's ratio have been explored by a number of researchers [1,5,14]. An overview of well-established techniques can be found in [11]. Typically additional degrees of freedom are added to the model by incorporating beams, angular springs and other custom three- or four-node connections which react not only to stretching, but shearing or applying torque as well. Introducing such elements allows to obtain wide range of

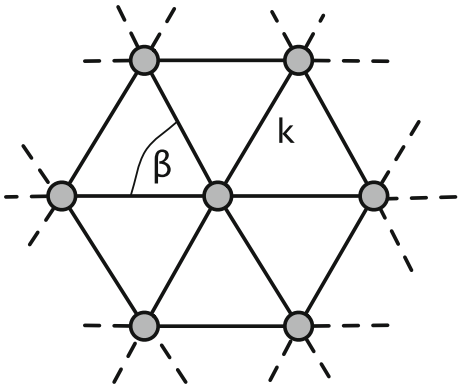

Fig. 3 Hexagonal lattice with normal as well as angular springs

materials; however, as volumetric objects are inherently more complex than two-dimensional structures, the description of their properties tends to be more complex as well. Analytical solutions are in most cases too difficult to derive and obtaining desirable properties of such models often involves a numerical minimization and parameter fitting that tunes the model to the particular problem at hand. This fact, together with increased computational and memory costs, makes such models less suitable for computer graphics or virtual reality applications.

In contrast, in this work we explore an approach of constructing MSM which allows to achieve arbitrary values of ν without introducing additional structures into the model. Our approach in fact makes use only of nodes and their relative pairwise distances.

3 Extended mass spring models

Simple MSMs described in Sect. 2 can be viewed as a network in Fig. 4. Forces in such networks act along straight lines between particles and this leads to $\nu = 1/4$, which may be considered a geometric property of the space (the way distance to neighboring nodes changes, when we change the position of a node).

We generalize this model by introducing an additional phenomenon. When two nodes approach, they start repelling each other as usual, and additionally each of them starts radiating momentum in "random" directions.

To visualize how we can justify such behavior, let us consider a particle–carrier interaction model where constituents of the matter (particles) interact with each other by means of exchanging carriers (which in turn can be considered a small particles). Carriers interact with particles (and with each other) by means of central forces (elastic collisions); therefore, this model still uses central forces as most basic means of interaction. Carriers, however, have a finite velocity so the transfer of momentum does not happen instantaneously; the big particles move as well. Having this in mind, we may

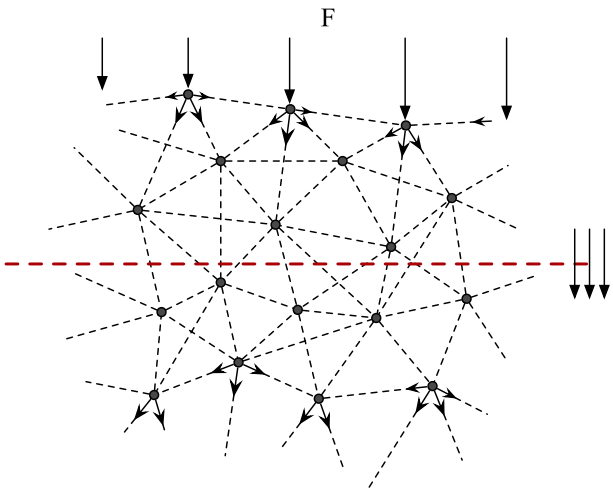

Fig. 4 Momentum flow through a simple MSM

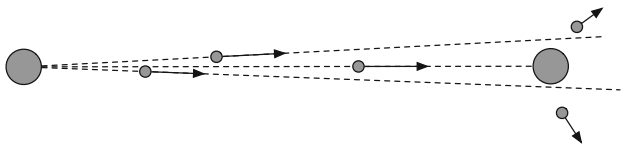

Fig. 5 Momentum dispersion

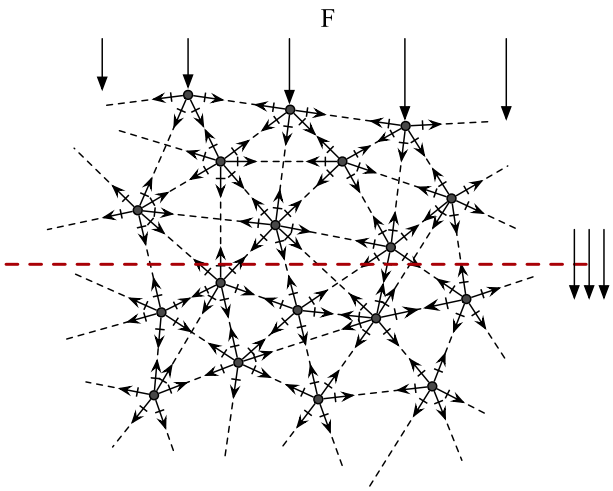

Fig. 6 Dispersive momentum flow

assume that a carrier shot form one particle, may not hit the other particle with a sniper's precision. In such case it will disperse in a "random" direction and will not come back to the first particle (Fig. 5). If a particle is bombarded from all directions uniformly, the dispersed carriers will also appear to be radiating from the particle uniformly (even if the actual distribution of dispersion angles is not trivial).

Figure 6 illustrates the dissipative part of the interaction, where each node absorbs the incoming carriers and radiates them uniformly in all directions. Such network will behave like a gas or fluid with no viscosity.

The standard expression for the stress in an elastic body

$$\sigma_{ij} = K\delta_{ij}\epsilon_{kk} + 2\mu\left(\epsilon_{ij} - \frac{1}{3}\delta_{ij}\epsilon_{kk}\right), \tag{5}$$

can be rewritten, by treating our material as a superposition of Cauchy's isotropic structure, in which $\lambda = \mu$ with a "fluid" in which $\sigma_{ij} = B\epsilon_{kk}\delta_{ij}$, where $B\epsilon_{kk}$ corresponds to pressure:

$$\sigma_{ij} = \mu\delta_{ij}\epsilon_{kk} + 2\mu\epsilon_{ij} + B\delta_{ij}\epsilon_{kk}, \quad B = \lambda - \mu \tag{6}$$

$$\sigma_{ij} = \frac{5}{3}\mu\delta_{ij}\epsilon_{kk} + 2\mu\left(\epsilon_{ij} - \frac{1}{3}\delta_{ij}\epsilon_{kk}\right) + B\delta_{ij}\epsilon_{kk}, \tag{7}$$

and the equation of motion becomes:

$$\rho\frac{\partial^2\bar{u}}{\partial t^2} = B\nabla(\nabla\cdot\bar{u}) + \mu(\nabla^2\bar{u} + 2\nabla(\nabla\cdot\bar{u})), \tag{8}$$

where $\bar{u}$ is a displacement and ρ is mass density.

The direct interactions correspond to μ parameter, dispersive ones to B. Both can be controlled, which allows to achieve other values of Poisson's ratio:

$$\nu = \frac{B+\mu}{2(B+2\mu)} = \frac{1+\frac{5}{3}Q}{2\left(2+\frac{5}{3}Q\right)}, \quad Q = \frac{B}{\frac{5}{3}\mu}, \tag{9}$$

where Q denotes the ratio between dissipative momentum flow and the direct one.

We incorporate the dispersion mechanism into MSMs by redistributing the fraction $q = 0.5Q$ of the incoming force at each node, to all the springs connected with it. The multiplication by the factor of 2 is introduced for convenience (one spring connects two nodes).

This task is, however, not as simple as accumulating and redistributing the actual force present on the springs. The springs in the network are in general not of equal lengths and their angular distribution is not strictly isotropic on per node basis. Because of that, the problem of accumulating and redistributing the force does require additional attention and the actual algorithm needs to properly scale influences of particular springs. Below we show how to construct extended MSM (eMSM) for two classes of networks. First, for lattice-based network with an exact analytical description of its properties (cubic lattice MSM), second, for disordered MSM, whose properties are statistical.

4 Extended cubic lattice MSM

For the cubic lattice MSM, we can explicitly calculate the equations of motion of the network (following the same procedure as [4]). From these equations we can deduce appropriate "q" coefficients for all springs.

The network which we consider is the cubic lattice network described in Sect. 2. Each node is connected with $b = 18$ neighboring nodes by springs of lengths L_i and spring coefficients κ.

Let us consider Taylor series in the displacement of neighboring nodes n and neighbors i of those as well:

$$u_{n\alpha} = u_\alpha + x_D\nabla_D u_\alpha + \frac{x_D x_E}{2}\nabla_D\nabla_E u_\alpha + \cdots \tag{10}$$

$$u_{ni\alpha} = u_{n\alpha} + x_{iB}\nabla_{iB}u_{n\alpha} + \frac{x_{iB}x_{iC}}{2}\nabla_{iB}\nabla_{iC}u_{n\alpha} + \cdots \tag{11}$$

The displacement of node i relative to node n is denoted as $\bar{u}_{ni}$. The displacement of node n relative to the central node is denoted as $\bar{u}_n$. The displacement of the central node is denoted as $\bar{u}$; its α coordinate is denoted as u_α. Similarly $\bar{x}$ denotes relative position of nodes and $\hat{x}$ is the unit vector in the direction of $\bar{x}$. The total force exerted on a central node can be decomposed to a direct interaction force F^μ and dispersive one F^*:

$$\bar{F} = \bar{F}^\mu + \bar{F}^* \tag{12}$$

The direct component is given by

$$\bar{F}^\mu = -\kappa\sum_{n=1}^{b}[(\bar{u} - \bar{u}_n)\cdot\hat{x}_n]\hat{x}_n, \tag{13}$$

where we sum the influences from all $b = 18$ neighbors. It can be approximated as

$$F^\mu_\alpha = \kappa\sum_{n=1}^{b}\frac{1}{2x_n^2}x_{n\alpha}x_{n\beta}x_{n\gamma}x_{n\delta}\nabla_\beta\nabla_\gamma u_\delta + O(\nabla^4 u), \tag{14}$$

which results in:

$$F_\alpha = \kappa a^2(\delta_{\alpha\beta}\delta_{\gamma\delta} + \delta_{\alpha\gamma}\delta_{\beta\delta} + \delta_{\alpha\delta}\delta_{\beta\gamma})\nabla_\beta\nabla_\gamma u_\delta, \tag{15}$$

where a denotes the length of the edge of an elemental cube. This gives the equations of motion which are isotropic in the large scale limit:

$$\rho\partial_t^2\bar{u} = \frac{\kappa}{a}(2\nabla\nabla\cdot\bar{u} + \nabla^2\bar{u}), \tag{16}$$

and in such case $\lambda = \mu = \kappa/a$. ρ is the mass density.

The dispersive component in turn is given by

$$F^* = -\sum_{n=1}^{b} g_n^* z_n\hat{x}_n, \tag{17}$$

where z_n is the momentum inflow from direct connections:

$$z_n = \kappa \sum_{i=1}^{b} G_i^*(\bar{u}_n - \bar{u}_{ni}) \cdot \hat{x}_{ni}. \tag{18}$$

Parameters g_n^* and G_i^* are meant to be adjusted to achieve a desirable network behavior.

This gives the approximation for the dispersive force

$$F_\alpha^* = \kappa \sum_{n=1}^{b} g_n^* \frac{x_{n\alpha}}{|x_n|} \sum_{i=1}^{b} G_i^* \frac{x_{niA}}{|x_{ni}|} (x_{iB} x_C \nabla_{iB} \nabla_C + \frac{x_{iB} x_{iC}}{2} \nabla_{iB} \nabla_{iC}) u_A. \tag{19}$$

If we take $G_i^* = q/L_i$ and $g_n^* = L_n/b$, where L_j is the natural length of jth spring and b is the number of springs connected to a node, we get:

$$F_\alpha^* = \frac{10}{3} q\kappa a^2 \delta_{\alpha C} \delta_{BA} \nabla_B \nabla_C u_A \tag{20}$$

$$\rho \partial_t^2 \bar{u} = \frac{10 q\kappa}{3a} \nabla\nabla\bar{u}, \tag{21}$$

and $Q = 2q$. Note that taking $G_i^* = qL_i$ and $g_n^* = 1/bL_n$ gives the same result and these are the coefficients that we will in fact be using (they give better behavior for large deformations of the networks which we are using).

This gives the desired total force acting on a node

$$F_\alpha = [(\mu + B)\delta_{\beta\alpha}\delta_{\gamma\delta} + \mu(\delta_{\gamma\alpha}\delta_{\beta\delta} + \delta_{\delta\alpha}\delta_{\beta\gamma})]\nabla_\beta \nabla_\gamma u_\delta. \tag{22}$$

[B defined as in Eq. (6)].

The obtained equations show that each spring in this network contributes $\kappa \Delta L_i q L_i$ to the momentum inflow J_{acc} of a node and receives J_{acc}/bL_i of it back as the dispersed outflow.

In other words, the force propagation algorithm which allows to obtain the desired behavior of the network may be constructed as follows:

For each node:

- Compute forces from springs $\bar{F}_i^\mu = -\kappa \Delta L_i$ (and apply them to the nodes).
- Additionally accumulate $-F_i^\mu q L_i$ on each node as J_{acc}.

In the second pass:

- Redistribute the accumulated force as $F^* = J_{\text{acc}}/bL_i$ to all the springs connected with the node.

5 Disordered eMSM

In case of disordered networks the relation $q(Q)$ cannot be determined so easily because it depends on the internal structure of the network. However, it turns out that using the same force propagation mechanism as in case of cubic lattice MSMs, we can achieve a desired behavior of disordered networks as well.

To show that the technique derived for cubic MSM works for disordered MSM as well, let us consider the influence of a single spring on the total bulk modulus of the material. Even though the springs are one-dimensional structures, they are used to model three-dimensional object and the force they exert is meant to act not only on a distance but also through two-dimensional surface (giving a pressure). Let us imagine then, that each spring represents a spherical[1] region of the material with radius $R = 0.5L$.

The bulk modulus of a spherical object can be calculated with

$$K = -V \frac{\mathrm{d}p}{\mathrm{d}V}.$$

Decreasing the radius of the sphere by ΔR induces the tension in the spring equal to $2k\Delta R$, hence the total pressure acting on the surface of the sphere becomes $p = 4k\Delta R/4\pi R^2$ whereas the relative change in the volume is $\Delta V/V = -3\Delta R/R$. This gives

$$K = \frac{k}{3\pi R}, \tag{23}$$

$$KV = \frac{4kR^2}{9} = \frac{kL^2}{9} \tag{24}$$

[note Eq. (3)]. The influence of the dispersive component can be in turn obtained by considering that $J_{\text{acc}} = \sum_j q k_j \Delta L_j / L_j$ is redistributed on each spring[2] as J_{acc}/bL_i:

$$K_i^* = 2\frac{2/bL_i}{\pi L_i^2 \cdot 3\Delta L_i/L_i} \sum_j q L_j^2 k_j \Delta L_j / L_j. \tag{25}$$

In uniform compression $\Delta L_i/L_i = \Delta L_j/L_j$. Moreover, $\sum_j q k_j L_j^2 = bq\langle kL^2\rangle$, where $\langle\rangle$ denotes the average over the springs connected to the node. This gives

$$K^*V = \frac{2q\langle kL^2\rangle}{9} \tag{26}$$

as the contribution of the dispersive component to the total K for a spring and approximately achieves the desired ratio $K^*/K = Q$ for the network.

[1] Any other shape can be used.

[2] Keep in mind that two nodes will contribute to the final value of the force on one spring, hence multiplication by two below.

6 Tests

To estimate numerically the value of ν in an MSM, we perform a numerical experiment in which a block of material is compressed in one direction, and the resulting deformation in other directions is measured. As we recall Poisson's ratio is the ratio of transverse to axial strain under uniaxial stress condition, i.e., $\nu = -\epsilon_{yy}/\epsilon_{xx}$, in an experiment where all components of the stress tensor are zero except σ_{xx}. It is problematic to guarantee this last condition and in practice we assume that other stress components may be non-zero as well. In such case ϵ_{yy} can be treated as a superposition of deformations caused by each of principal stress components:

$$\epsilon_{yy} = \frac{1}{E}[\sigma_{yy} - \nu(\sigma_{xx} + \sigma_{zz})], \tag{27}$$

or in general case:

$$\epsilon_{ii} = \frac{1}{E}[\sigma_{ii}(1+\nu) - \nu(\sigma_{11} + \sigma_{22} + \sigma_{33})]. \tag{28}$$

This allows to estimate ν accounting for the effects of non-uniaxial stress in the body, e.g.,

$$\nu = \frac{\epsilon_{xx}\sigma_{yy} - \epsilon_{yy}\sigma_{xx}}{\epsilon_{xx}(\sigma_{xx} + \sigma_{yy}) - \epsilon_{yy}(\sigma_{xx} + \sigma_{zz})}. \tag{29}$$

Additionally, to avoid various problems related to the measurement near border regions, the value of ν was measured as average ν from Eq. (29) in a specific region in the center of the block. The width of this region was set to 80 % of the width of the block. Stress measurements were carried out using Hardy's method [2,15], and strain by comparing positions of points in deformed and undeformed body. The initial block dimensions were $70a_0 \times 15a_0 \times 15a_0$ (where a_0 is an arbitrary unit of length) and the base spring constant has been set to k_0. The static displacement in x direction was imposed on all the nodes on the boundary of the block (allowing the points still to move in YZ plane).

The results of the experiment are presented in Figs. 7 and 8 and they confirm that any value of Poisson's ratio can be achieved with a high accuracy (within classical limits of its value, that is from -1 to 0.5). The differences between measurements and theoretical predictions are within limits of the measurement error of our measurement techniques for almost all tested materials and MSM resolutions (as long as the resolution is high enough to allow to construct a stable network that may be considered homogeneous).

Additionally, Fig. 9 presents pictures of compressed cuboid block made from four different materials with Poisson's ratio equal to -1, 0, 0.25 and 0.47. Their responses to compression are visibly different, showing how materials with various ν deform under directional compression (note

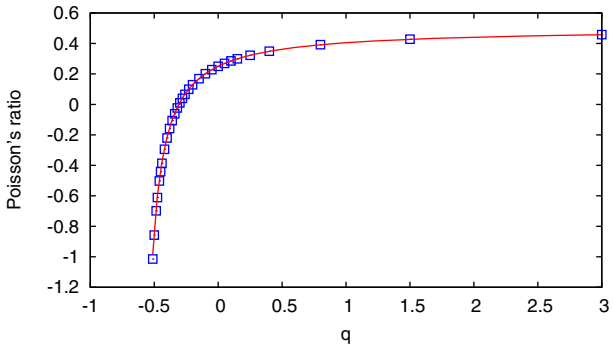

Fig. 7 Poisson's ratio in cubic lattice MSM. *Red curve* represents a theoretical prediction. *Blue points* are the results of measurements

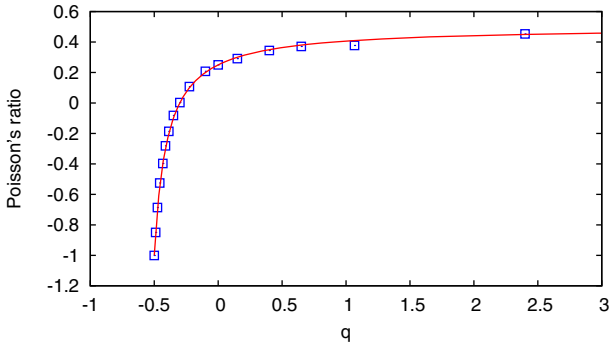

Fig. 8 Poisson's ratio in random MSM. *Red curve* represents a theoretical prediction. *Blue points* are the results of measurements

that border conditions in this test case are different than in the previous one; here the displaced points are not allowed to move in the YZ plane).

Although these shapes are very simple, the tests show that our extended MSM is capable of modeling bulk materials accurately. Given sufficiently high resolution, any complex shape can be modeled reliably. Figure 10 shows a deformation of a rabbit when its head is pulled back with a force. The two presented models have the same elastic properties but different resolutions. Figure 11 shows a deformation of an armadillo model, where the force was applied to the armadillo's arm and the resulting deformation calculated across cubic and random models with different resolutions. These figures, demonstrate that the change of resolution does not affect the elastic properties noticeably (in contrast to models presented in [1] or [12]). Deformations like these (deflections caused by constant force), however, do not depend on Poisson's ratio in an obvious way, which can be seen on the Fig. 12. The effects of changing ν are much better visible in compression or stretching experiments such as the one presented in the Fig. 13. It should be noted, however, that the change of Poisson's ratio does require a corresponding change in bulk modulus if we want to keep, e.g., the Young's modulus constant. For the model from Fig. 13, where $E = 200\ k_0/a_0$, it means that spring stiffness coeffi-

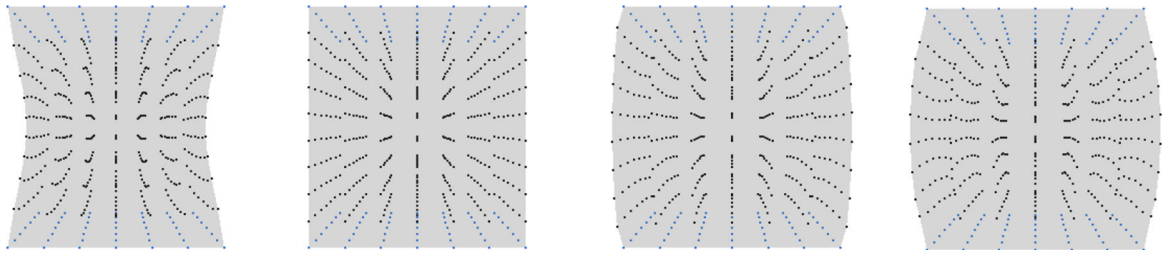

Fig. 9 A block of material with dimensions $2 \times 3 \times 2$ compressed in y direction to 75 % of its natural length. Different values of Poisson's ratio, from the *left* -1, 0, 0.25, 0.47

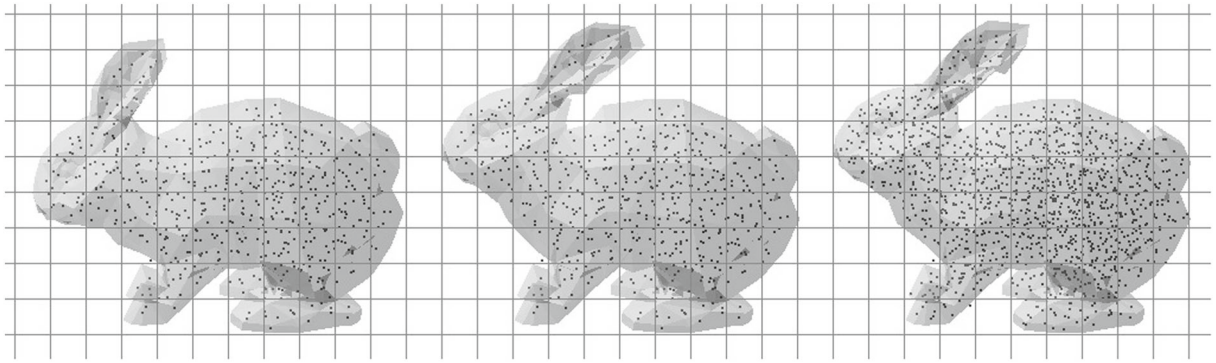

Fig. 10 A force is applied to the head of a rabbit, pulling it backwards. Poisson's ratio of the material is set to $\nu = 0$. *Left* undeformed model, *middle* low-res random MSM 581 nodes, 4903 springs, *right* mid-res random MSM 1321 nodes 12,085 springs. The model is provided courtesy of Princeton Shape Benchmark repository

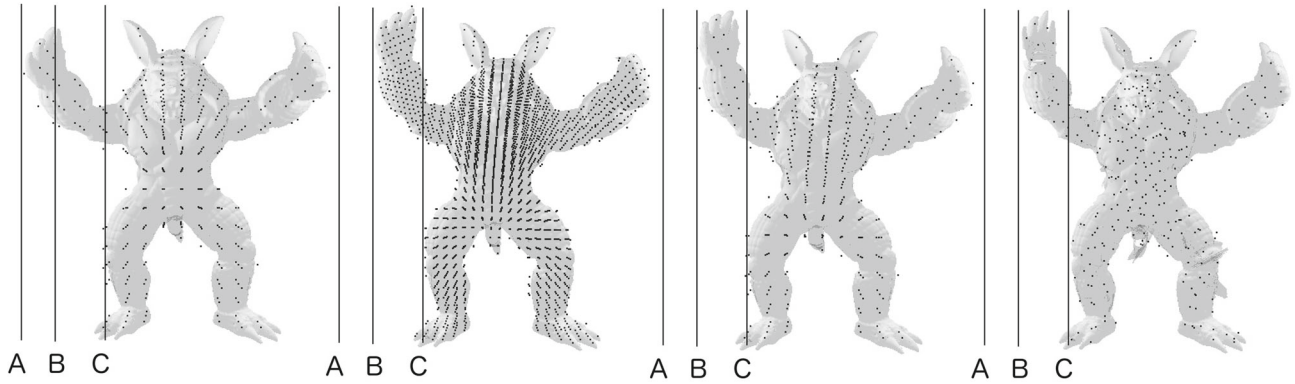

Fig. 11 A force is applied to the armadillo's arm. *Lines A*, *B* and *C* show undeformed and deformed positions of high-resolution model. Poisson's ratio of the material is set to $\nu = 0.33$. From the *left* (1) Undeformed model, (2) hi-res cubic MSM 3813 nodes 27,110 springs, (3) mid-res cubic MSM 779 nodes, 4796 springs, (4) low-res random MSM 315 nodes, 1906 springs. The model is provided courtesy of The Stanford 3D Scanning Repository

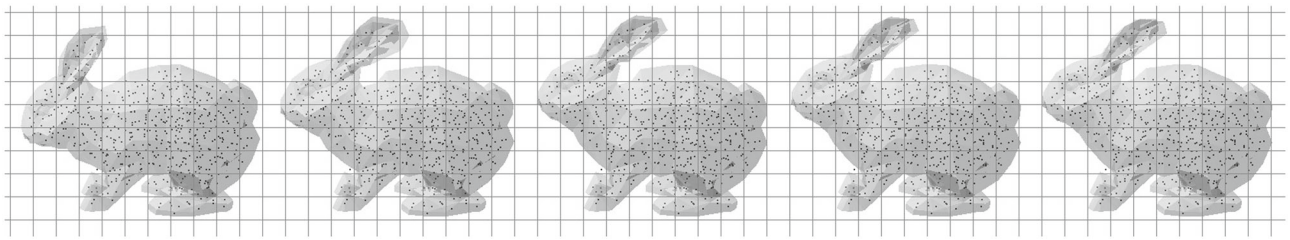

Fig. 12 Same as Fig. 10, but for different values of Poisson's ratio. From the *left* Undeformed model, $\nu = -0.5$ model, $\nu = 0$ model, $\nu = 0.25$ model and $\nu = 0.4$ model

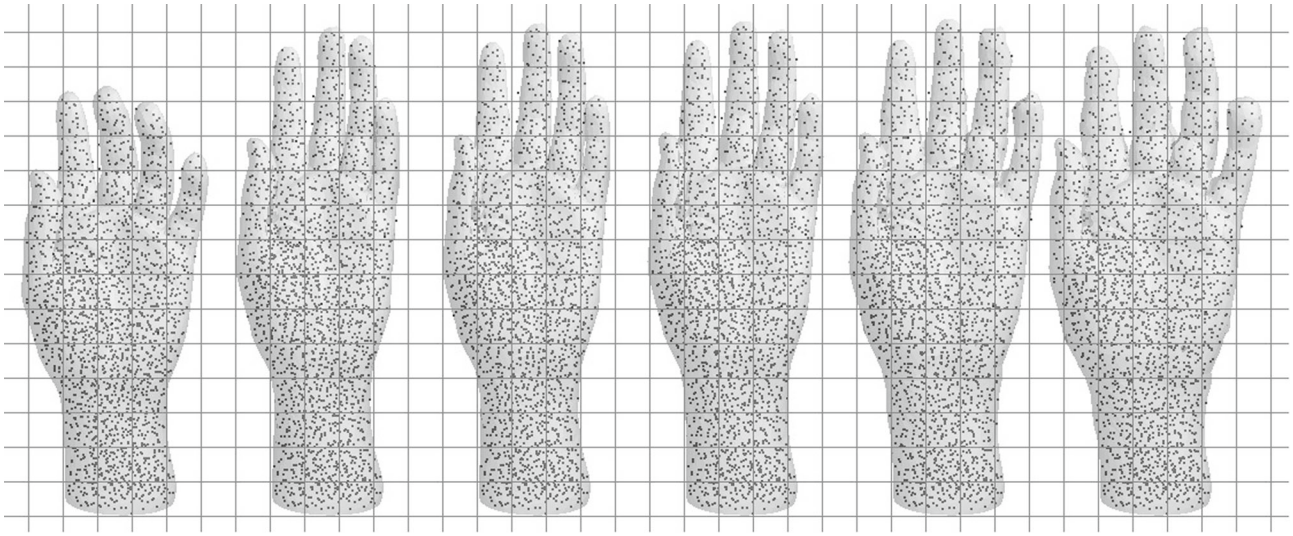

Fig. 13 A homogeneous material with the shape of a hand. Random MSM. From the *left* undeformed model, resulting deformation for $\nu = 0.49$, 0.25, 0.0, −0.5, −0.9. The model is provided courtesy of AIM@SHAPE-VISIONAIR Shape Repository

cients were set to $k = 67k_0$ ($\nu = -0.49$, $K = 3333\,k_0/a_0$), $k = 80\,k_0$ ($\nu = 0.25$, $K = 133\,k_0/a_0$), $k = 100\,k_0$ ($\nu = 0.0$, $K = 66\,k_0/a_0$), $k = 200\,k_0$ ($\nu = -0.5$, $K = 33\,k_0/a_0$), $k = 1000\,k_0$ ($\nu = -0.9$, $K = 23\,k_0/a_0$).

7 Conclusions

In this article we showed an approach of constructing MSM which allows to achieve arbitrary values of ν without introducing additional structures into the MSM. We demonstrated that by incorporating the concept of momentum dispersion, additional degree of freedom can be added to the classical MSM. This enables to freely represent homogeneous isotropic materials characterized by two different constants (in contrast to one constant description given by classical MSM). To our best knowledge no other MSM-like method can achieve the full spectrum of the values of Poisson's ratio.

Because our method does not introduce additional elements to the MSM itself, the memory costs remain unchanged and the computational costs rise by a relatively low degree when compared to simple MSM. The simplest implementation of our model, when used with explicit time integrator, requires additional iteration through all the springs in the system. When compared with simple MSM, this may double the time of the force computation if the performance is limited by memory access (likely to be the case in GPU computation). Some improvements are, however, possible; for instance the value of momentum dispersed on the nodes in the 'previous' frame could be used to approximate the value in the current frame. This eliminates the need of additional iteration through the springs, but may influence the stability of the simulation.

The existence of analytical description of our model (in particular in case of cubic lattice MSM) makes it an attractive starting point for developing more advanced models (e.g., for anisotropic materials). In current work, we have assumed that the dispersion of the force happens uniformly in all directions giving isotropic properties of the material; however, by introducing non-uniform dispersion mechanisms it should be possible to achieve non-isotropic behaviors without extensive modifications of the current model. Such modifications may be a good direction for the future work, as they would allow to efficiently model, e.g., organic tissues for surgical simulations.

Acknowledgments Authors acknowledge the support of JSPS KAKENHI (Grant Number 24300035).

Appendix: Useful relations

Dimensionality of the space is denoted by d.

$$K = \lambda + 2\mu/d \tag{30}$$

$$E = \frac{2\mu(\lambda d + 2\mu)}{(d-1)\lambda + 2\mu} \tag{31}$$

$$\nu = \frac{\lambda}{(d-1)\lambda + 2\mu} \tag{32}$$

$$\mu = \frac{E}{2(1+\nu)} \tag{33}$$

$$\mu = \frac{K \cdot d \cdot (1 + \nu(1-d))}{2(1+\nu)} \tag{34}$$

$$\lambda = \frac{K \cdot d \cdot \nu}{1+\nu} \tag{35}$$

$$Q = \frac{\lambda - \mu}{(1 + 2/d)\mu} \tag{36}$$

References

1. Baudet, V., Beuve, M., Jaillet, F., Shariat, B., Zara, F.: Integrating Tensile Parameters in 3D Mass-Spring System. Technical Report RR-LIRIS-2007-004, LIRIS UMR 5205 CNRS/INSA de Lyon/Université Claude Bernard Lyon 1/Université Lumiére Lyon 2/École Centrale de Lyon (2007)
2. Hardy, R.J.: Formulas for determining local properties in molecular-dynamics simulations - Shock waves. J. Chem. Phys. **76**, 622–628 (1982)
3. Kot, M., Nagahashi, H., Szymczak, P.: Elastic moduli of simple mass spring models. Vis. Comput. **31**(10), 1339–1350 (2015)
4. Ladd, A.J.C., Kinney, J.H.: Elastic constants of cellular structures. Phys. A Stat. Theor. Phys. **240**(1–2), 349–360 (1997)
5. Lakes, R.S.: Deformation mechanisms in negative Poisson's ratio materials: structural aspects. J. Mater. Sci. **26**, 2287–2292 (1991)
6. Liu, T., Bargteil, A.W., O'Brien, J.F., Kavan, L.: Fast simulation of mass-spring systems. Proceedings of ACM SIGGRAPH Asia 2013, ACM Transactions on Graphics, vol. 32(6), pp. 209:1–7. Hong Kong (2013)
7. Love, A.E.H.: A treatise on the mathematical theory of elasticity. Cambridge University Press, Cambridge (1906)
8. Nealen, A., Müller, M., Keiser, R., Boxerman, E., Carlson, M., Ageia, N.: Physically based deformable models in computer graphics. Comput. Graph. Forum **25**(4), 809–836 (2006)
9. Ostoja-Starzewski, M.: Lattice models in micromechanics. Appl. Mech. Rev. **55**(1), 35–60 (2002)
10. Press, W.H., Teukolsky, S.A., Vetterling, W.T., Flannery, B.P.: Numerical Recipes 3rd Edition: The Art of Scientific Computing, 3rd edn. Cambridge University Press, New York (2007)
11. Sahimi, M.: Rigidity and Elastic Properties: The Discrete Approach. In: Heterogeneous Materials: Linear Transport and Optical Properties. Interdisciplinary Applied Mathematics vol. 1, (Chapter 8). Springer, New York (2003)
12. San-Vicente, G., Aguinaga, I., Celigueta, J.T.: Cubical mass-spring model design based on a tensile deformation test and nonlinear material model. IEEE Trans. Vis. Comput. Graph. **18**(2), 228–241 (2012)
13. Van Gelder, A.: Approximate simulation of elastic membranes by triangulated spring meshes. J. Graph. Tools **3**(2), 21–42 (1998)
14. Zhao, G.-F., Fang, J., Zhao, J.: A 3d distinct lattice spring model for elasticity and dynamic failure. Int. J. Numer. Anal. Methods Geomech. **35**(8), 859–885 (2011)
15. Zimmerman, J.A., Webb III, E.B., Hoyt, J.J., Jones, R.E., Klein, P.A., Bammann, D.J.: Calculation of stress in atomistic simulation. Model. Simul. Mater. Sci. Eng. **12**(4), S319 (2004)

Maciej Kot received his M.Sc. degree in Computer Science from Warsaw University of Technology and an M.Sc. degree in physics from the University of Warsaw in 2010. In 2014, he received a Ph.D. degree in Computer Science from Tokyo Institute of Technology Imaging Science and Engineering Laboratory where he now conducts a postdoctoral research. His research interests include computer graphics and physical-based modeling and simulation.

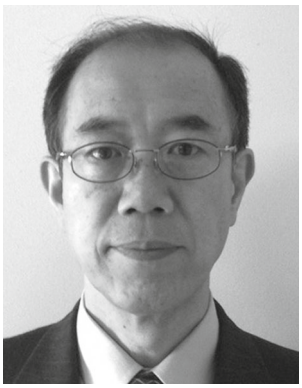

Hiroshi Nagahashi received his B.E. and Ph.D. degree from Tokyo Institute of Technology in 1975 and 1980, respectively. Since 1990, he has been working with Imaging Science and Engineering Laboratory at Tokyo Institute of Technology, where he is currently a professor. His research interests include computer vision, computer graphics, and geometric modeling.